

Analytical Solution of Laminar Forced Convection in a Heated Channel Subjected to Reciprocating Flow

By

A.M.A. Regeb & A.K.M Alshara
Department of Mechanical Engineering
Engineering College, University of Basrah, Basrah Iraq.
September 20, 2007

Abstract

Hydrodynamics and heat transfer in a fully developed laminar incompressible reciprocating channel flow subjected to a constant heat flux have been investigated analytically using similarity transformation. An exact analytical solution for the velocity, local and bulk temperature as well as of Nusselt number have been obtained. The effect of the parameters Pr, A_0, λ and X/D_h on u^+, T^+, T_b^+, Nu_x and \overline{Nu}_x are presented.

The results showed that the local Nusselt number is increased with increasing Womersly number (λ) while the dimensionless temperature is increased with Womersly and decreased with amplitude (A_0). Prandtl number has significant effect on local Nusselt number.

The results were found in very good agreement with that obtained numerically using finite volume method. The comparison with the experimental results of other authors gave a reasonable identification.

Keywords: Similarity solution; Reciprocating flow; Heat transfer; Channel

الحل التحليلي للحمل القسري الطبقي في قناة

موضوعه تحت جريان ترددي

أ.د. عبد المحسن عبود رجب & د. أحمد كاظم محمد الشرع

قسم الهندسة الميكانيكية

كلية الهندسة - جامعة البصرة

20 أيلول 2007

الخلاصة

تمت دراسة تحليلية لهيدروديناميكية و انتقال الحرارة في جريان تام التشكيل طبقي غير أنضغاطي وترددي في قناة موضوعه تحت فيض حراري ثابت باستخدام التحويلات المتماثلة. تم الحصول على الحل التحليلي التام للسرعة ودرجة الحرارة الموضوعية والمعدل ورقم نسلت. تأثير المتغيرات X/D_h و λ, Pr, A_0 على

u^+, T^+, T_b^+, Nu_x و \overline{Nu}_x قد تم تمثيلها.

النتائج بينت بأن رقم نسلت الموضوعي يزداد مع زيادة رقم ومورسلي بينما درجة الحرارة الأبعدية تزداد مع ومورسلي وتتناقص مع السعة. رقم براندل له تأثير واضح على رقم نسلت. النتائج وجدت بتطابق جيد مع النتائج العددية باستخدام الحل العددي بطريقة الحجم المتناهية والمقارنة مع نتائج عملية لباحثين آخرين أعطت تطابق معقول.

Nomenclature

- A_0 Dimensionless oscillation amplitude, X_{\max} / D_h
 c Specific heat of fluid, $J / \text{kg} \cdot \text{K}$
 D_h Hydraulic diameter, $4H, m$
 f Similarity transformation function, $u^+ = f(y^+)e^{i\omega t}$
 g Similarity transformation function defined in eq.(15)
 H Half height of channel, m
 h_x Local heat transfer coefficient, $W / m^2 \cdot K$
 k Thermal conductivity, $W / m \cdot K$
 L Length of channel, m
 Nu_x Local Nusselt number
 p Pressure of the fluid, N / m^2
 Pr Prandtl number, ν / α
 P_0 Amplitude of pressure gradient of the fluid, m / s^2
 q'' Heat flux at the wall, W / m^2
 Re_ω Kinetic Reynolds number, $\omega D_h^2 / \nu$
 t Time, s
 T Temperature, K
 u Axial velocity, m / s
 \bar{u}_m Time – space averaged axial velocity, m / s
 x Axial distance, m
 X_{\max} Maximum amplitude of the fluid displacement, m
 y Vertical coordinate for channel, m
 α Thermal diffusivity of fluid, m^2 / s
 β_{crit} Critical values of reciprocating flow, $(A_0 \sqrt{Re_\omega})_{\text{crit}}$
 γ Dimensionless time average axial temperature gradient, $\frac{d\bar{T}_b^+}{dx^+}$
 λ Womersly number, $H\sqrt{\omega/\nu}$
 μ Dynamic viscosity of fluid, $\text{kg} / m \cdot s$
 ν Kinematic viscosity of fluid, m^2 / s
 ρ Density of fluid, kg / m^3
 τ Dimensionless time, ωt
 ω Radial oscillatory frequency, rad / s

Subscript

- b Bulk
 c Center line
 max Maximum value
 w Wall
 x Axial distance

Superscript

- $+$ Dimensionless
 $-$ Time average

Introduction

Oscillatory flow is important in the modern life and can be found in many fields such as biological, sociology, engineering application such as I.C. and Stirling engines and design of heat exchangers. Reciprocating flow is the first type of oscillatory flow in which the mean velocity is equal to zero, the other type is the pulsating flow where the mean velocity is not equal to zero. Reciprocating flow can be found in Stirling cycles machines, pulse tube cryocooler, heat exchangers, electronic cooling and pulse combustor. The requirements of these equipments to have an optimum and best design conditions necessitate the development of these studies.

The unsteady flow is simply occurred when the motion of the fluid is started suddenly from rest. The flow near a flat plate which are impulsively accelerated from the rest was solved firstly by Stokes as cited by Schlichting [1]. The similar case for suddenly accelerated flow from rest is the flow about an infinite flat wall which executes linear harmonic oscillations parallel to itself and which was first treated by Stokes and later by Rayleigh as cited by [1]. They found that the oscillatory boundary layer or the so called 'Stokes layer' has thickness of

$\delta = \sqrt{2\nu/\omega}$ which increased with increasing the kinematics viscosity and decreasing with increasing the angular frequency. This showed that the thickness of boundary layer became thinner with increasing the frequency, which lead to enhance the characteristics of oscillatory flow.

Uchida^[2] 1956, obtained an exact solution for axial velocity profile of a fully developed laminar reciprocating flow in a circular pipe. This solution was simplified to give the velocity distribution for small values of the Womersly number (very low oscillation) and large values of Womersly number (very high oscillation).

Many of experimental studies were made to describe the oscillatory flow characteristics. Zhao & Cheng^[3], investigated analytically and experimentally the fully developed laminar incompressible reciprocating pipe flow. They defined the cycle-averaged friction coefficient as a function of the kinetic Reynolds number and the amplitude. Karagoz^[4] 2002, introduced analytical solution based on similarity transformation for oscillatory pressure driven, fully developed flow in a channel. Variations of the velocity profile and skin friction coefficient over a cycle had been obtained together

with behavior of the flow for various oscillation frequencies.

Most heat transfer studies in reciprocating flow are experimental or numerical and only few analytical can be found. Kurzweg^[5], considered the heat transfer rate between two reservoirs by conduction only and the effect of reciprocating flow on the coefficient of thermal diffusivity. Kurzweg^[6] examined analytically the enhancement of longitudinal heat transfer through a sinusoidally oscillatory viscous flow in array of parallel-plate channels with conducting side walls.

Zhao and Cheng^[7] 1995, presented a numerical solution for laminar forced convection of an incompressible periodically reversing flow in a pipe of finite length at constant wall temperature. They illustrated a typical phase shifts between temperature and axial velocity at selected locations. Karagoz^[8] studied numerically and experimentally the boundary layer of heated channel from the bottom. He illustrated the effect of Reynolds and Womersly numbers on the heat transfer parameters. Sert and Beskok^[9] 2003, performed a numerical simulation for reciprocating flow in two-dimensional channels. The flow between two parallel plates was considered harmonically in time with a pressure gradient. They

observed the quasi-steady flow behavior for $\alpha=1$ (where $\alpha = H\sqrt{\omega/\nu}$) (low frequency), and Richardson's effect for $\alpha=10$ (high frequency).

It is clear that there are many numerical and experimental studies carried out for this type of flow but there is a scare in analytical investigation. In this type of flow, there are many difficulties to find analytical solution for the hydrodynamic and heat transfer in reciprocating flows due to the complicated nature of unsteady flows. Therefore this study will be devoted to solve analytically the reciprocating flow in order to understand the phenomenon of the unsteady flow and the controlling parameters. In this study a new analytically solution is developed using similarity transformation for momentum and energy equations and as a checking means, a numerical solution applying finite volume method is also obtained. The effect of the parameters (λ , Pr , X/D_h and A_o) are taken in to account in evaluation of the velocity profile, local and bulk temperature distribution and local Nusselt number.

Theoretical Analysis

1- Hydrodynamics analysis

The reciprocating flow in the 2D channel Fig.1, is analyzed

hydrodynamically. The Navier-Stokes equations for fully developed flow, constant properties, reciprocating pressure driven and laminar flow through a horizontal channel can be written as

$$-\frac{1}{\rho} \frac{\partial p}{\partial y} = 0 \quad (1)$$

$$\frac{\partial u}{\partial t} = -\frac{1}{\rho} \frac{\partial p}{\partial x} + \nu \frac{\partial^2 u}{\partial y^2} \quad (2)$$

where^[2]

$$-\frac{1}{\rho} \frac{\partial p}{\partial x} = P_o \cos \omega t \approx \text{Re}(P_o e^{i\omega t}) \quad (3)$$

The boundary and initial conditions

$$1. u = 0 \text{ at } y = \pm H \text{ for } t > 0$$

no slip at th wall (4a)

$$2. \frac{\partial u}{\partial y} = 0 \text{ at } y = 0 \text{ for } t > 0$$

axisymmetric (4b)

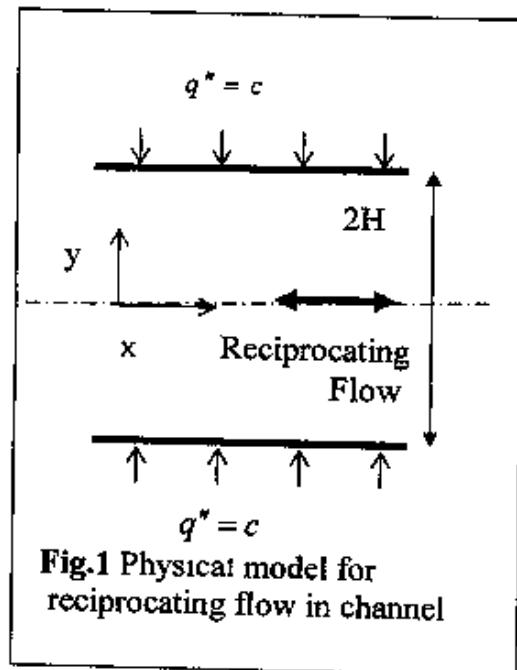
$$3. u = f(y) \text{ at } t = 0$$

initial condition (4c)

In dimensionless form Eq.2 can be written as

$$\frac{\partial u^+}{\partial t^+} = e^{i t^+} + \frac{1}{\lambda^2} \frac{\partial^2 u^+}{\partial y^{+2}} \quad (5)$$

The boundary and initial conditions in dimensionless form becomes



$$1. u^+ = 0 \text{ at } y^+ = \pm 1 \text{ } t^+ > 0 \quad (6a)$$

$$2. \frac{\partial u^+}{\partial y^+} = 0 \text{ at } y^+ = 0 \text{ } t^+ > 0 \quad (6b)$$

$$3. u^+ = f(y^+) \text{ at } t^+ = 0$$

initial condition (6c)

where

$$u^+ = \frac{u}{u_{\max}}, \quad u_{\max} = \frac{X_{\max} \omega}{2} = \frac{P_o}{\omega},$$

$$\lambda = H \sqrt{\omega / \nu} = \frac{1}{4} \sqrt{\text{Re}_w}, \quad \text{Re}_w = \frac{D_h^2 \omega}{\nu},$$

$$y^+ = \frac{y}{H}, \quad t^+ = \omega t \text{ and } D_h = 4H$$

(for the channel with width \gg height)

Applying similarity transformation of the form^[5] $u^+ = f(y^+) e^{i t^+}$ in Eq.5 gives

$$f'' - i \lambda^2 f = -\lambda^2 \quad (7)$$

Solving the above ordinary differential equation yields

$$f = i \left[\frac{\cosh \sqrt{i} \lambda y^+}{\cosh \sqrt{i} \lambda} - 1 \right] \quad (8a)$$

and

$$u^+ = i \left[\frac{\cosh \sqrt{i} \lambda y^+}{\cosh \sqrt{i} \lambda} - 1 \right] e^{u^+} \quad (8b)$$

Applying the identity $\sqrt{i} = \frac{1+i}{\sqrt{2}}$,

the real part of u^+ can be written as

$$u^+ = \frac{(C^2 + D^2 - AC - BD) \sin t^+}{C^2 + D^2} - \frac{(BC - AD) \cos t^+}{C^2 + D^2} \quad (9)$$

where

$$A = \cosh(\lambda y^+ / \sqrt{2}) \cos(\lambda y^+ / \sqrt{2}) \quad (10a)$$

$$B = \sinh(\lambda y^+ / \sqrt{2}) \sin(\lambda y^+ / \sqrt{2}) \quad (10b)$$

$$C = \cosh(\lambda / \sqrt{2}) \cos(\lambda / \sqrt{2}) \quad (10c)$$

$$D = \sinh(\lambda / \sqrt{2}) \sin(\lambda / \sqrt{2}) \quad (10d)$$

2- Heat transfer analysis

Taking into account the previous assumptions the problem can be described by energy equation without viscous dissipation ($\Phi=0$) which could be reduced to^[2]

$$\frac{\partial T}{\partial t} + u \frac{\partial T}{\partial x} = \alpha \frac{\partial^2 T}{\partial y^2} \quad (11)$$

The boundary and initial conditions are

$$1. \frac{\partial T}{\partial y} = 0 \quad \text{at } y = 0 \quad \text{for } t > 0$$

axisymmetric (12a)

$$2. q'' = k \frac{\partial T}{\partial y} \quad \text{at } y = \pm H \quad \text{for } t > 0,$$

const. heat flux at the wall (12b)

$$3. T = f(y) \quad \text{at } t = 0$$

initial condition (12c)

Eq.11 in the dimensionless form becomes

$$\text{Pr} \lambda^2 \frac{\partial T^+}{\partial t^+} + \frac{1}{2} A_o \text{Pr} \lambda^2 u^+ \frac{\partial T^+}{\partial x^+} = \frac{\partial^2 T^+}{\partial y^{+2}} \quad (13)$$

where

$$\text{Pr} = \frac{\mu c_p}{k}, T^+ = \frac{kT / D_h}{q''}, x^+ = \frac{x}{D_h}$$

$$\text{and } A_o = \frac{X_{\max}}{D_h}$$

and $D_h = 4h$ (for the channel with width \gg height)

The boundary conditions become:

$$1. \frac{\partial T^+}{\partial y^+} = 0 \quad \text{at } y^+ = 0 \quad \text{for } t^+ > 0$$

axisymmetric (14a)

$$2. \frac{\partial T^+}{\partial y^+} = 1 \quad \text{at } y^+ = \pm 1 \quad \text{for } t^+ > 0$$

const. heat flux at the wall (14b)

$$3. T^+ = \gamma(x^+ + g(y^+)) \quad \text{at } t^+ = 0$$

initial condition (14c)

Assuming similarity transformation of the form⁽⁶⁾

$$T = \frac{d\bar{T}_b}{dx} (x + D_h g(y) e^{i\omega t}) \quad (15)$$

or in dimensionless form yields

$$T^+ = \frac{d\bar{T}_b^+}{dx^+} (x^+ + g(y^+) e^{i\omega^+}) = \gamma (x^+ + g(y^+) e^{i\omega^+}) \quad (16)$$

where: $\frac{d\bar{T}_b^+}{dx^+}$ is a time-average axial dimensionless temperature gradient and

$$\bar{T}_b^+ = \frac{1}{\pi} \int_0^\pi T_b^+ dt^+ \quad (17a)$$

where

$$T_b^+ = \frac{\int_0^1 T^+ u^+ dy^+}{\int_0^1 u^+ dy^+} \quad (17b)$$

Substituting the similarity transformation of T^+ Eq.16, and the solution of u^+ Eq.8b in Eq.13, then the energy equation described by Eq.13 can be reduced to ordinary differential equation as

$$g'' - i \text{Pr} \lambda^2 g = \frac{i A_o \text{Pr} \lambda^2}{2} \left[\frac{\cosh \sqrt{i \lambda} y^+}{\cosh \sqrt{i \lambda}} - 1 \right] \quad (18)$$

The solution of Eq.18 can be written as

$$g = C_1 \cosh \sqrt{i \text{Pr} \lambda} y^+ + C_2 \sinh \sqrt{i \text{Pr} \lambda} y^+ + \frac{A_o \text{Pr}}{2(1-\text{Pr})} \frac{\cosh \sqrt{i \lambda} y^+}{\cosh \sqrt{i \lambda}} + \frac{A_o}{2} \quad (19)$$

where C_1 and C_2 are constants.

Using the boundary conditions described by equations Eqs.14a and 14b yield the temperature distribution

$$T^+ = \gamma \left[x^+ + \frac{E_1 + F_1}{U_2 \sqrt{2 \text{Pr} \lambda} \gamma} - \frac{A_o \text{Pr}}{2 \sqrt{\text{Pr}} (1-\text{Pr})} \left(\frac{(E_1 Y_1 - F_1 Z_1) \cos t^+}{U_2 C_3} - \frac{(E_1 Z_1 + F_1 Y_1) \sin t^+}{U_2 C_3} \right) + \frac{A_o \text{Pr}}{2} * \left(\frac{Q_1 \cos t^+ - P_1 \sin t^+}{C_3 (1-\text{Pr})} + \frac{\cos t^+}{\text{Pr}} \right) \right] \quad (20)$$

where

$E_1, F_1, U_2, Y_1, Z_1, C_3, Q_1$ and P_1 are functions obtained during derivation and given in the Appendix A.

The gradient of dimensionless time-average bulk temperature γ used in the previous derivation can be obtained from the energy balance for control volume of the fluid in the channel as

$$2q'' \cdot l \cdot dx = \rho c_p (2H \cdot l) \bar{u}_m d\bar{T}_b \quad (21)$$

or in dimensionless form

$$\frac{d\bar{T}_b^+}{dx^+} = \frac{4\nu}{Pr H \bar{u}_m} \quad (22)$$

where \bar{u}_m is obtained from the following relation

$$\bar{u}_m = \frac{1}{\pi} \int_0^\pi u_{\max} \sin \phi \, d\phi = \frac{2u_{\max}}{\pi} \quad (23)$$

thus Eq.22 can be written as

$$\frac{d\bar{T}_b^+}{dx^+} = \gamma = \frac{\pi}{4 Pr A_o \lambda^2} \quad (24)$$

The instantaneous-local Nusselt number is defined as

$$Nu_x = \frac{h_x \cdot D_h}{k} = \frac{l}{T_w^+ - T_b^+} \quad (25)$$

where

$$h_x = \frac{q''}{(T_w - T_b)}$$

while the time averaged -local Nusselt number is defined as

$$\bar{Nu}_x = \frac{\bar{h}_x \cdot D_h}{k} = \frac{l}{\bar{T}_w^+ - \bar{T}_b^+} \quad (26)$$

where

$$\bar{T}_w^+ = \frac{1}{\pi} \int_0^\pi T_w^+ dt^+ \quad (27)$$

Results and Discussion

The solution of momentum and energy equations shows that four parameters have influence on the flow and heat transfer and these are: Womersly number λ , dimensionless amplitude of fluid displacement A_o , Prandtl number Pr and the ratio of distance to hydraulic diameter x/D_h .

The values of λ and A_o are to be taken so that the value of $A_o \sqrt{Re_w}$ is not greater than $\beta_{crit}^{[2]}$. To avoid the limit of turbulence intensity region, the values of β_{crit} are taken to be less or equal to 400 as most authors used^[2], and the values of λ and A_o are then related to it. The Prandtl number Pr is taken to equal 0.7 in the various calculations.

Reciprocating flow require interchange between the inflow and out flow boundaries along the length of pipe or channel during a cycle. It is assumed that the fluid particles during a cycle exiting the flow domain, i.e. the time required for the flow to go along the channel length equal to the time for the coming back flow.

Starting from the velocity distribution, Fig.2 illustrates the variation of dimensionless velocity u^+ with dimensionless channel height during a half cycle π . The velocity profile is represented at

different times (30° between each time used). The profiles clarify that the velocity is depending on the time at which the velocity is taken for constant controlling parameters. Therefore at a certain time the u^+ becomes parabolic (unidirection) and in other time it reverse specially at the region near the wall. This effect is due to the oscillation of the flow which makes the region near the wall faster than at the core region and this is called Richardson annular effects^[2]. At approximately 130° the flow begins to reverse its direction (the fluid flowing near the wall starts to reverse its direction as much as 30° approximately sooner than the flow reversal in the center of the channel.

Fig.3 shows the distribution of dimensionless temperature T^+ with dimensionless channel height over a half cycle π . It is clear from the temperature profiles, that the wall temperature is greater than the center temperature since the heating is at the wall. The sharp velocity gradient near the wall leads to change in the temperature distribution across the channel height, i.e. the annular effect of velocity creates annular effect in the temperature distribution. It is also clear from the shape of velocity and temperature distributions that, increasing the

velocity causes a decrease in the temperature.

The two Figs. 2 & 3 show the phase shift between the velocity and temperature distributions.

Figs.4 & 5 indicate the influence of Womersly number λ on the velocity u^+ profile and temperature T^+ profile respectively across the channel height at the dimensionless time $\pi/3$. For high Womersly number λ of flow, the velocity and temperature distribution is significantly affected by the Richardson's annular effect.

Fig.6 & 7 present the effects of Womersly number λ and dimensionless amplitude of the fluid displacement A_0 on the bulk temperature T_b^+ over a complete cycle 2π . Fig.6 illustrates the influence of increasing Womersly number λ on T_b^+ during a one cycle 2π . The values of λ are equal to: 4, 8, and 12. It shows declining in T_b^+ with increasing Womersly number, because of increasing the velocity of flow due to increase the frequency, which cause the temperature to decrease. The effect of dimensionless amplitude of fluid displacement A_0 on the bulk temperature T_b^+ along one cycle 2π is presented in the Fig.7. It is illustrated that T_b^+ decreases with increasing A_0 , which is due to

increase of quantity of flow (velocity or volumetric flow rate) with increasing A_0 .

The periodical change of the velocity with time for reciprocating flow requires that the velocity at the certain time reaches zero which, makes the dimensionless bulk temperature T_b^+ to go to infinity at that time. This behavior makes a clear discontinuity in the distribution of T_b^+ with time.

Fig.8 indicates the variation of instantaneous-local Nusselt number Nu_x with time (one cycle 2π) for different value of Womersly number ($\lambda = 4, 8$ and 12). The increment of Womersly number raises Nu_x , which is attributed to thinner boundary layer and therefore small thermal resistance. The values of Nu_x goes to infinity at the certain time, which is resulting from the value of T_b^+ . It is clearly shown from the figure that the value of Nu_x for reciprocating flow is larger than that for steady fully developed flow in the channel which equals to $\overline{Nu} = 8.235^{[11]}$. This enhancement makes the application of oscillatory flow or reciprocating flow is very effective means for enhancement of heat transfer and can be used in a wide field of industrial application.

Fig.9 illustrates the effect of dimensionless amplitude of fluid displacement A_0 on the local Nusselt number Nu_x over a one cycle 2π . It is shown that A_0 has no effect on Nu_x , because the variation of A_0 means the change of velocity or volumetric flow rate which has no effect on Nu_x for fully developed flow.

Fig.10 illustrates the variation of the instantaneous-local Nusselt number Nu_x over one cycle 2π for different x/D_h ($x^+ = 10, 20$ & 25) and the other parameters are constant. It is seemed from the figure that Nu_x is independent on x/D_h , since the flow is fully developed.

Finally, the variation of the time averaged-local Nusselt number \overline{Nu}_x with Pr number during one cycle 2π , is presented in the Fig.11, for two values of λ ($\lambda = 4$ and 8) while the other controlling parameters are kept constant. The increment of Prandtl number Pr increases \overline{Nu}_x due to the change of thermophysical properties of the fluid. Also, the figure shows the effect of Womersly number λ on the time averaged-local Nusselt number \overline{Nu}_x , which increases with increasing the Womersly number λ .

Eq.5 is solved numerically using the finite volume method. Fig.12 shows the comparison between analytical and numerical solution of Eq.5, which gives a very good agreement. Fig.13 illustrates the analytical and numerical solution of τ^+ (solution of Eq.13). This figure shows a very good agreement between analytical and numerical models. In the region near the wall a less agreement is obtained, because of the annular effect or the oscillation flow which is occurred in the region nearest to the wall.

The new model is compared with experimental investigation for convective heat transfer in a rectangular duct heated from below and subjected to a periodic flow, by Copper et al. and cited by Zhao and Cheng^[2]. This experimental work was done for turbulent flow and the results were correlated by suitable relation for \overline{Nu} since no experimental work done for laminar flow therefore the comparison will be made at critical oscillatory parameter β_{crit} only. The parameter that used in the comparison is space-cycle

averaged Nusselt number \overline{Nu} which is defined as^[2]

$$\overline{Nu} = 0.548 * A_n^{0.3} * Re_n^{0.536} \quad (28)$$

where

$$\lambda = \frac{1}{4} \sqrt{Re_n} \quad \text{for channel}$$

Fig.14 shows the comparison between the value of \overline{Nu} obtained from the new model with the experimental correlation obtained by Copper et al.^[2] (Eq.28) for various values of Womersly number. The behavior of the results obtained from both work have a similar trend. The observed difference between them may be attributed the flow region that used in the experimental correlation (transition and turbulent regions).

Conclusions

From the present analytical model it can be concluded that:

- 1- Analytical modeling for hydrodynamics and heat transfer in the oscillatory flow is possible based on the following considerations: laminar, 2D, incompressible, horizontal channel, no viscous dissipation $\Phi=0$ and the flow is driven by reciprocating pressure gradient.
- 2- The reciprocating flow is studied and the obtained effecting

parameters that control the flow and heat transfer are defined as: Womersly number λ , dimensionless amplitude of fluid displacement A_0 , Prandtl number Pr and the ratio of distance to hydraulic diameter x/D_h .

3- The dimensionless bulk or center temperature and the instantaneous-local Nusselt number Nu_x are fluctuating periodically with time.

4- The instantaneous-local Nusselt number Nu_x and time averaged-local Nusselt number \overline{Nu}_x are clearly increased with increasing Womersly number and Prandtl number.

5- The reciprocating flow gives enhancement in the heat transfer rate reaches to order of magnitude for Nu_x or \overline{Nu}_x as compared with steady state flow at the same considerations ($\overline{Nu}_x = 8.235$ without reciprocating flow).

References

[1] Schlichting H., "Boundary-Layer Theory", 7th Edition, McGraw-Hill, U.S.A., 1979.

[2] Zhao T.S. & Cheng P., "Heat Transfer in Oscillatory Flows", Annual Review of Heat Transfer, Vol. IX, Chapter 7, 1998.

[3] Zhao T.S. and Cheng P., "The Friction Coefficient of a Fully Developed Laminar Reciprocating Flow in a Circular

Pipe", Int. J. Heat and Fluid Flow, Vol.17, No.2, p.p.167-172, 1996.

[4] Karagöz İ., "Similarity Solution of the Oscillatory Pressure Driven Fully Developed Flow in a Channel", Uludağ Üniversitesi Mühendislik-Mimarlık Fakültesi Dergisi, Cilt7, Sayı 1, 2002.

[5] Kurzweg U.H., "Enhanced Heat Conduction in Fluids Subjected to Sinusoidal Oscillations", J. Heat Transfer, Vol. 107, pp.459-462, 1985.

[6] Kurzweg U.H., "Enhanced Heat Conduction in Oscillating Viscous Flows within Parallel-Plate Channels", J. Fluid Mech., Vol. 156, pp.291-300, 1985.

[7] Zhao T. & Cheng P., "A Numerical Solution of Laminar Forced Convection in a Heated Pipe Subjected to a Reciprocating Flow", Int. J. Heat Mass Transfer, Vol.38, No.16, pp.3011-3022, 1995.

[8] Karagoz I., "Variation of Momentum and Thermal Boundary Layers for Oscillatory Flows in a Channel", Int. Comm. Heat Mass Transfer, Vol.28, No.3, pp.379-388, 2001

[9] Sert C. and Beskok A., "Oscillatory Flow Forced Convection in Micro Heat Spreaders", Numerical Heat Transfer, Part A, Vol.42, pp.685-705, 2002.

[10] Sert C. and Beskok A., "Numerical Simulation of

Reciprocating Flow Forced convection in Two-Dimensional Channels", ASME J.Heat Transfer, Vol.125, pp.403-412, 2003.

[11] **Burmeister L. C.**, "Convective Heat Transfer", 1st Edition, John Wiley & Sons, 1983.

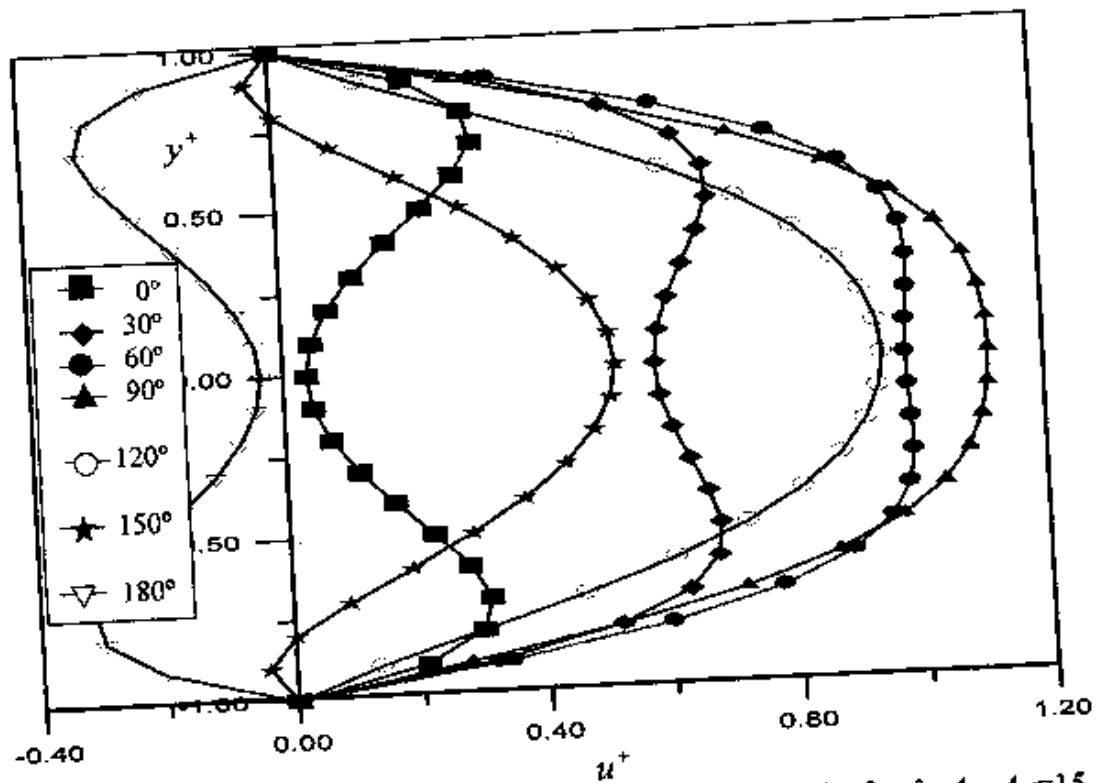


Fig.2 The Variation of the dimensionless velocity profile for $\lambda=4$, $A_0=15$, $Pr=0.7$ and $x/D_h=20$.

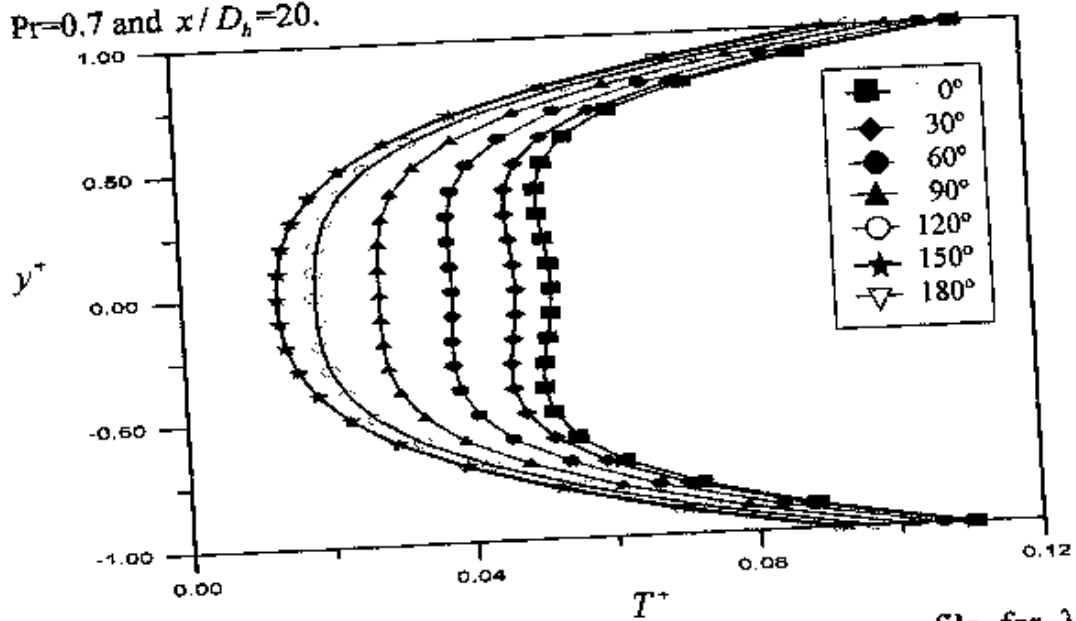


Fig.3 The Variation of the dimensionless temperature profile for $\lambda=4$, $A_0=15$, $Pr=0.7$ and $x/D_h=20$.

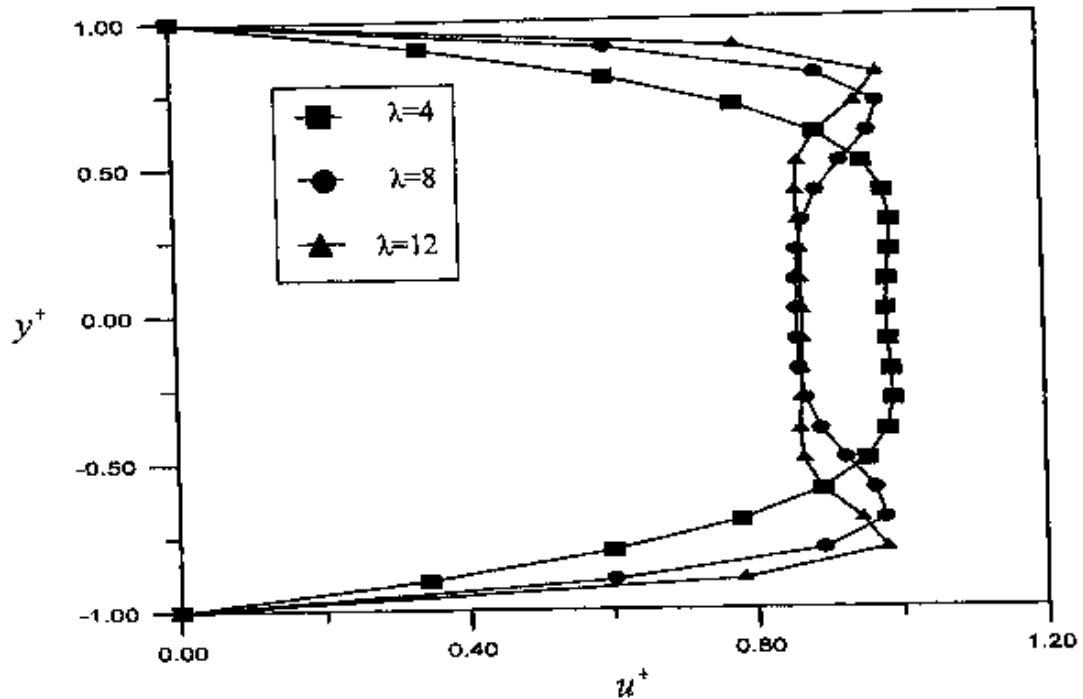


Fig.4 The Effect of Womersley number λ on the dimensionless velocity profile at $\omega t = 60^\circ$, for $A_0 = 15$, $Pr = 0.7$ and $x / D_h = 20$.

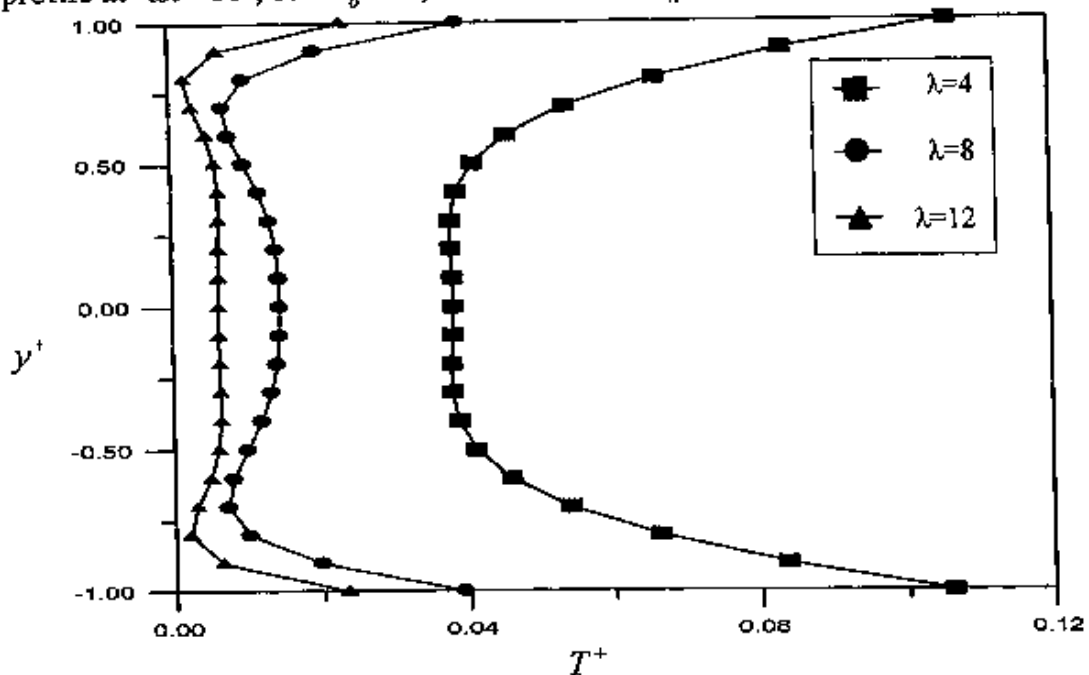


Fig.5 The Effect of Womersley number λ on the dimensionless temperature profile at $\omega t = 60^\circ$, for $A_0 = 15$, $Pr = 0.7$ and $x / D_h = 20$.

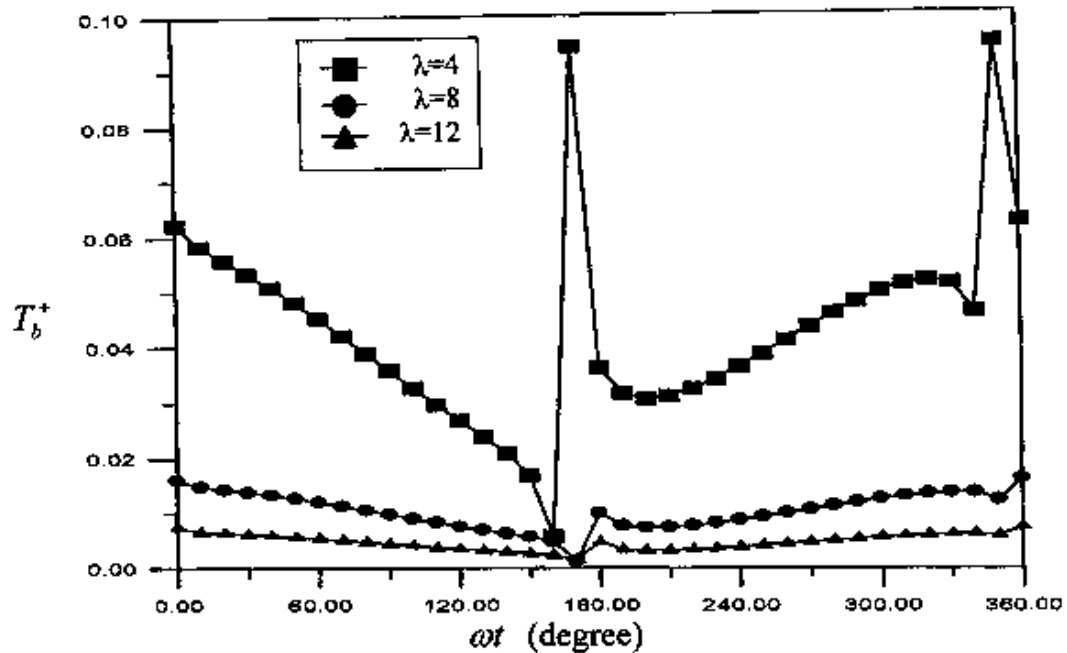


Fig.6 The Effect of Womersly number λ on the instantaneous dimensionless bulk temperature at $A_o=15$, $Pr=0.7$ and $x/D_h=20$.

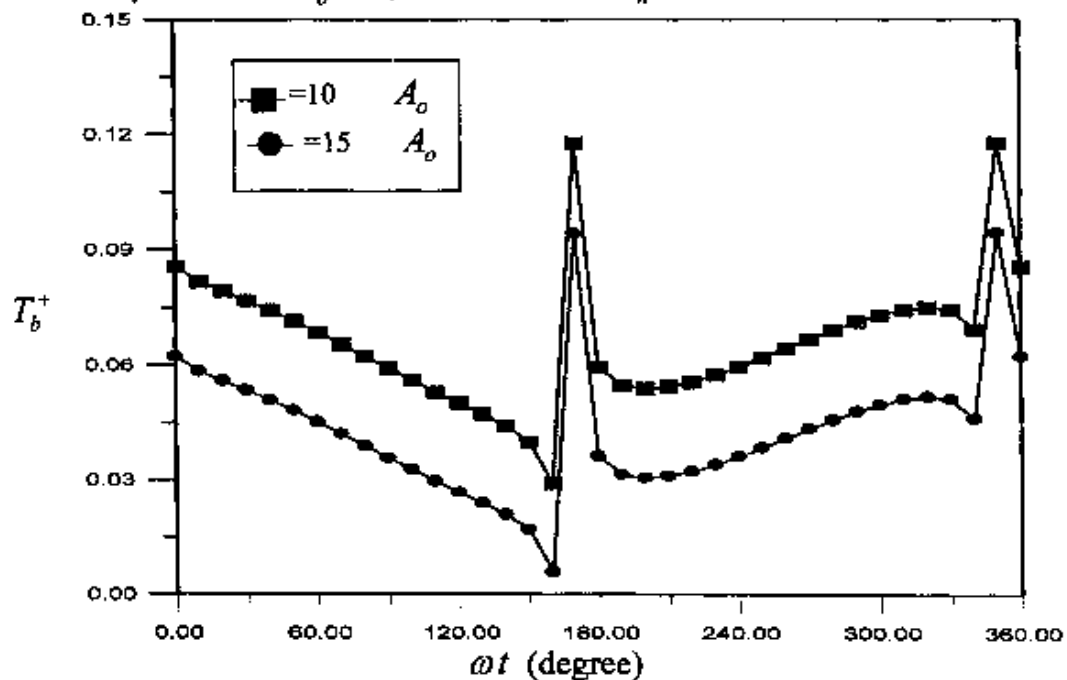


Fig.7 The Effect of dimensionless amplitude of fluid displacement on the instantaneous dimensionless bulk temperature at $\lambda=4$, $Pr=0.7$ and $x/D_h=20$.

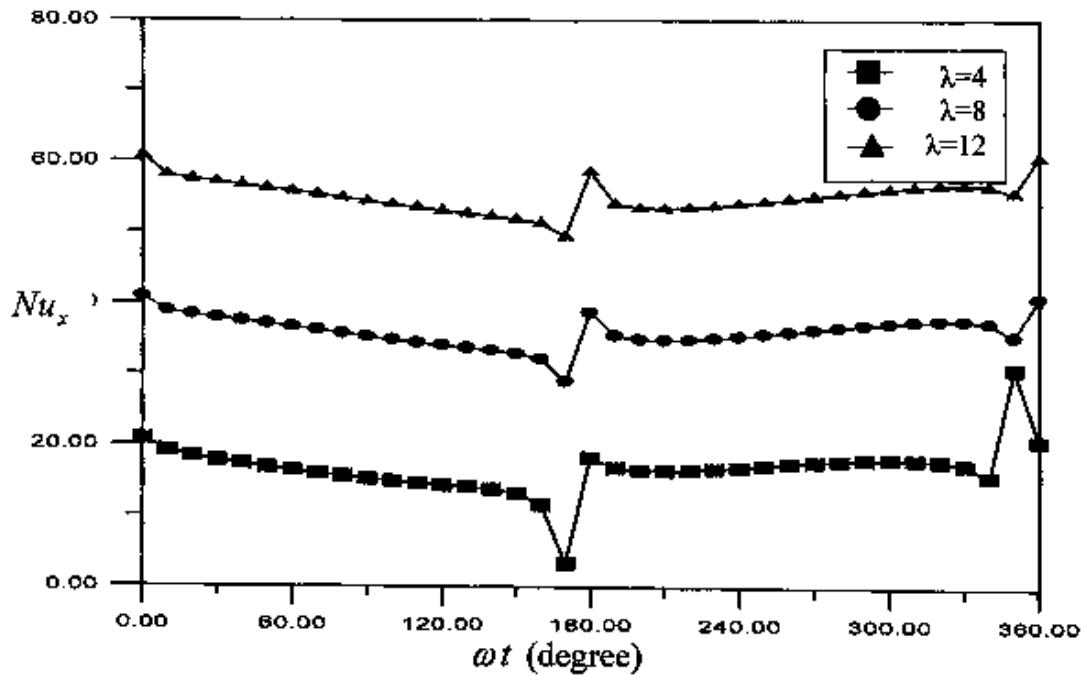


Fig.8 The Effect of Womersley number on the instantaneous-local Nusselt number at $A_o=15$, $Pr=0.7$ and $x/D_h=20$.

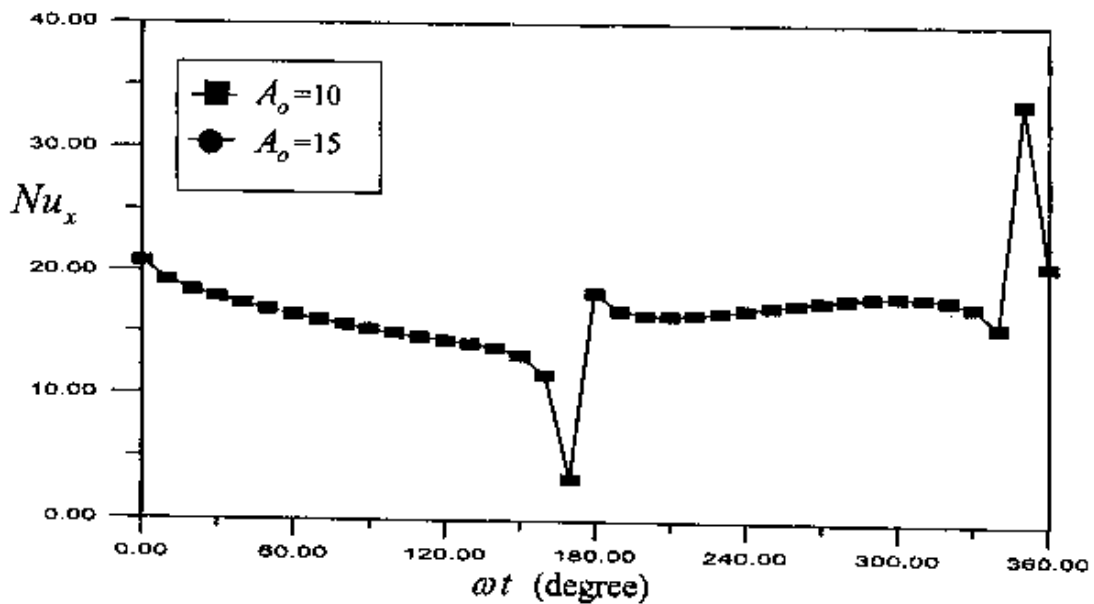


Fig.9 The Effect of dimensionless amplitude of fluid displacement on the instantaneous-local Nusselt number at $\lambda=4$, $Pr=0.7$ and $x/D_h=20$.

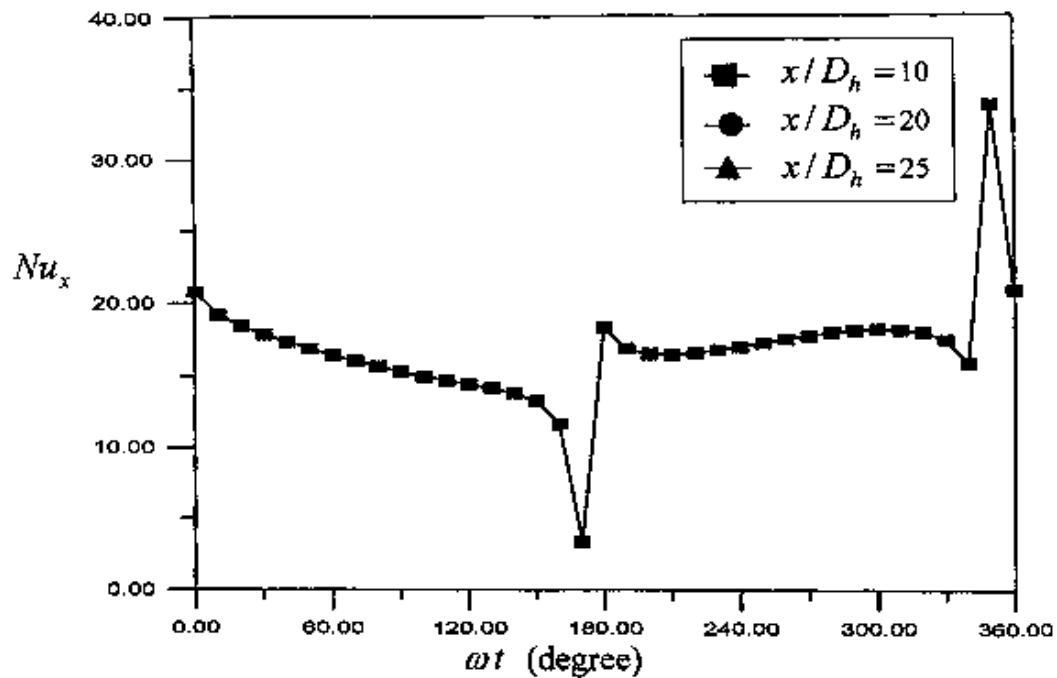


Fig.10 The Effect of ratio of the distance to the hydraulic diameter on the instantaneous-local Nusselt number at $\lambda=4$, $A_o=15$ and $Pr=0.7$.

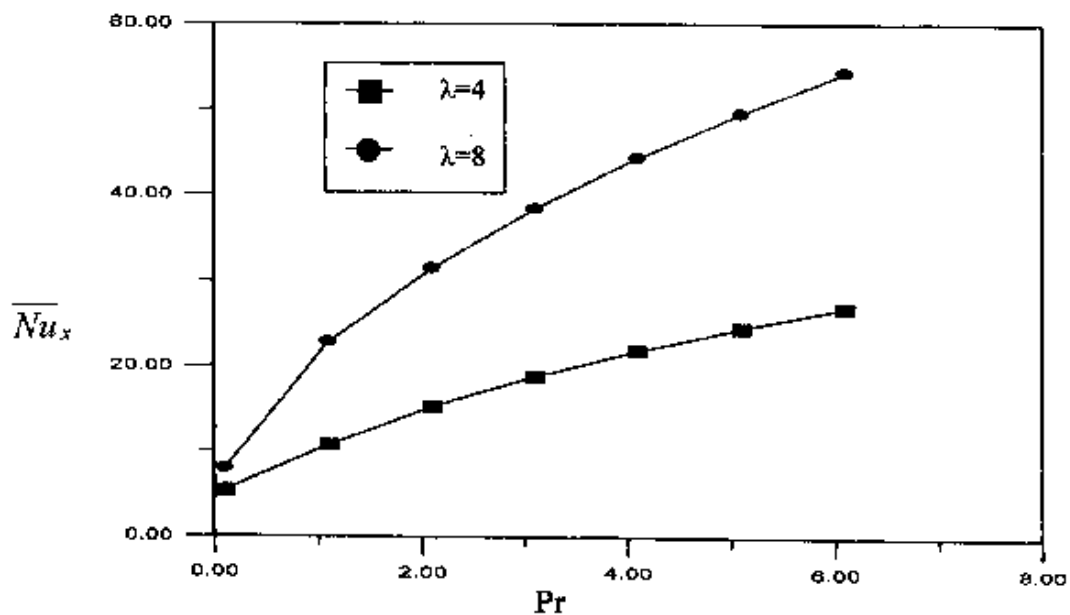


Fig.11 The Effect of Prandtl number on the time averaged-local Nusselt number at $\lambda=4$ and 8 , for $A_o=15$ and $x/D_h=20$.

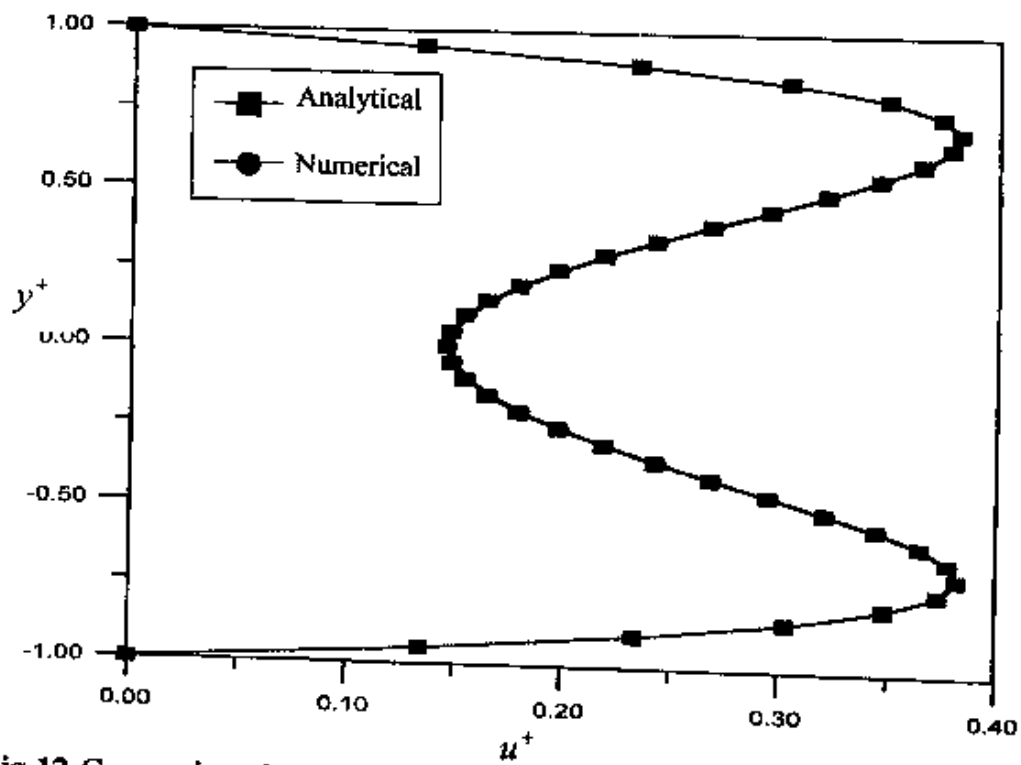


Fig.12 Comparison between the velocity profile of analytical and numerical solutions at $\omega t = 0.05$, $\lambda=4$, $A_o = 15$, $Pr=0.7$ and $x/D_h = 20$.

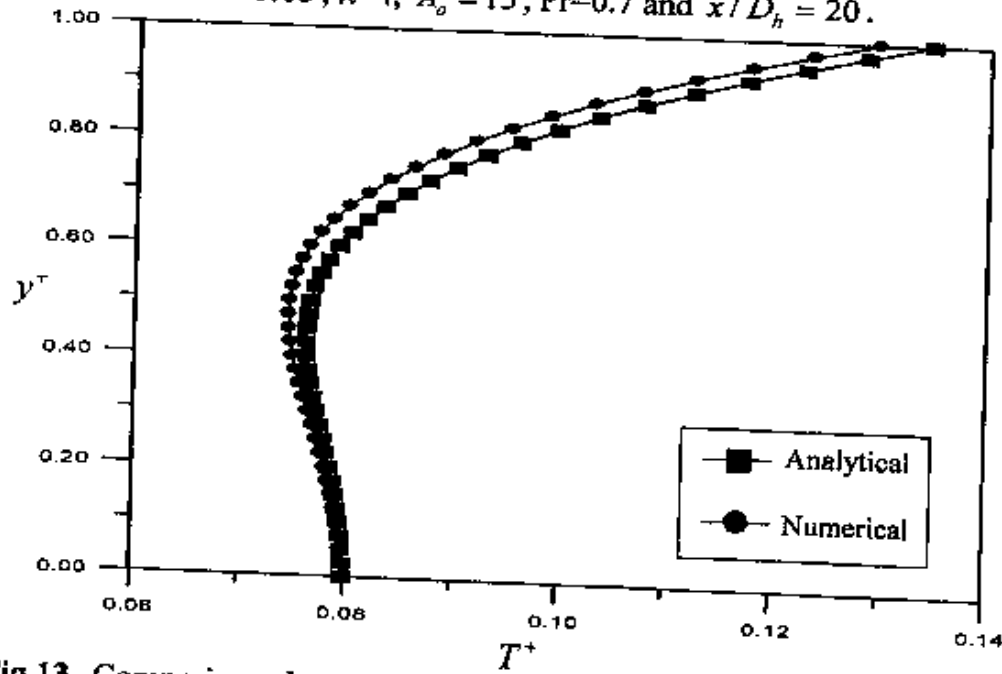


Fig.13 Comparison between the temperature profile of analytical and numerical solutions at $\omega t = 0.05$, $\lambda=4$, $A_o = 15$, $Pr=0.7$ and $x/D_h = 20$.

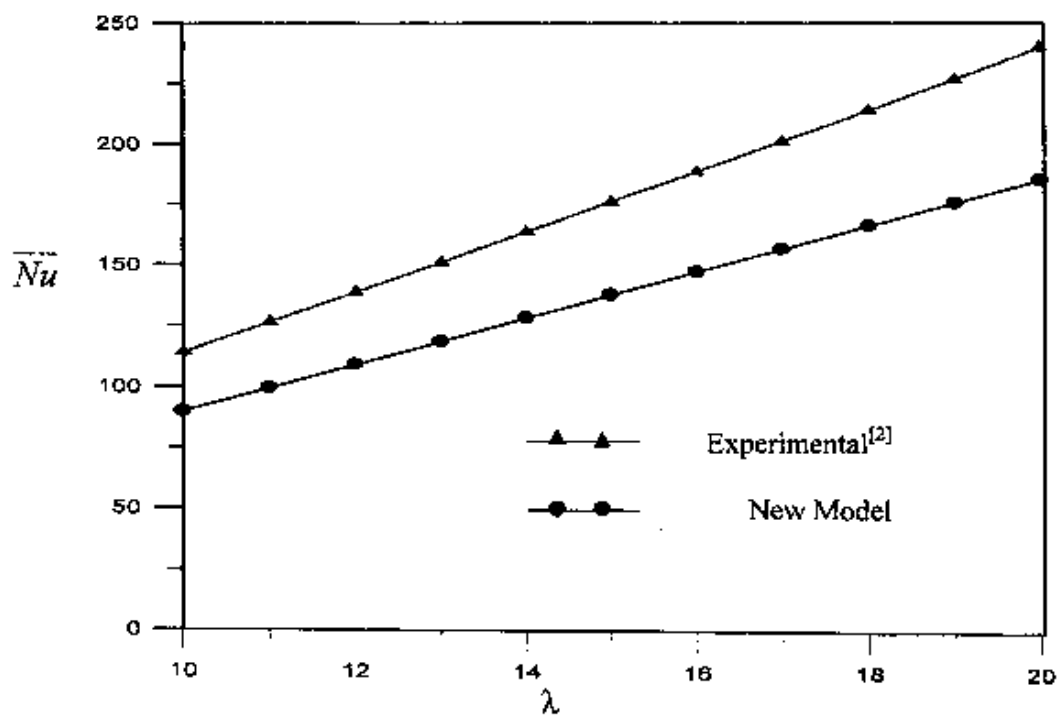


Fig.14 Comparison of the space-cycle averaged Nusselt number between present model and the experimental correlation of Copper et al.^[2].

Appendix A

The functions that find in the Eq.3.20 are defined as

$$E_1 = E U + F W \quad (A.1)$$

$$F_1 = F U - E W \quad (A.2)$$

$$U_2 = U^2 + W^2 \quad (A.3)$$

$$Y_1 = Y C + Z D \quad (A.4)$$

$$Z_1 = Z C - Y D \quad (A.5)$$

$$C_3 = C^2 + D^2 \quad (A.6)$$

$$Q_1 = Q C + P D \quad (A.7)$$

$$P_1 = P C - Q D \quad (A.8)$$

and

$$E = \cosh(\sqrt{Pr/2} \lambda y^+) \cos(\sqrt{Pr/2} \lambda y^+) \quad (A.9)$$

$$F = \sinh(\sqrt{Pr/2} \lambda y^+) \sin(\sqrt{Pr/2} \lambda y^+) \quad (A.10)$$

$$U = \sinh(\sqrt{Pr/2} \lambda) \sin(\sqrt{Pr/2} \lambda) \quad (A.11)$$

$$W = \cosh(\sqrt{Pr/2} \lambda) \cos(\sqrt{Pr/2} \lambda) \quad (A.12)$$

$$Q = \cosh(\lambda/\sqrt{2} y^+) \cos(\lambda/\sqrt{2} y^+) \quad (A.13)$$

$$P = \sinh(\lambda/\sqrt{2} y^+) \sin(\lambda/\sqrt{2} y^+) \quad (A.14)$$

$$C = \cosh(\lambda/\sqrt{2}) \cos(\lambda/\sqrt{2}) \quad (A.15)$$

$$D = \sinh(\lambda/\sqrt{2}) \sin(\lambda/\sqrt{2}) \quad (A.16)$$

$$Y = \sinh(\lambda/\sqrt{2}) \cos(\lambda/\sqrt{2}) \quad (A.17)$$

$$Z = \cosh(\lambda/\sqrt{2}) \sin(\lambda/\sqrt{2}) \quad (A.18)$$